Libyan Journal of Ecological & Environmental Sciences and Technology
(LJEEST)

LJEEST
ISSN: 2710-5237
www.srcest.org.ly/jou

http://aif-doi.org/LJEEST/040210

Determination of Change in Surface Waterbodies in The Middle Rio Grande Basin by Modified Normalized Difference Water Index (MNDWI) 1994-2020

Omar S Belhaj[1] Stanley T Mubako[2] Craig E Tweedie[3] Raed E Aldouri[4]
William L Hargrove[5] Elhadi A Hadia[6].

ARTICLE INFO

Vol.4 No.2 December, 2022
Pages (67- 80)

Article history:
Revised form 01 October 2022
Accepted 12 November 2022

Authors affiliation
1. Center for Environmental Resource Management, University of Texas at El Paso, College of Science, University of Elmergib, Khoms, Libya.
2. Division of Statewide Integrated Water Management, Land Use Unit- Water Use and Efficiency Branch, California Department of Water Resources.
3. Professor, Department of Biological Sciences, Director, Environmental Science and Engineering Program, University of Texas at El Paso.
4. Professor Civil Engineering Department, University of Texas at El Paso, Regional Geospatial Service Center, Director.
5. Former Director, Center for Environmental Resource Management, University of Texas at El Paso (now retired).
6. College of Science, University of Elmergib, Khoms, Libya.
obelhaj@miners.utep.edu
omarsolliman@gmail.com
Tel: 9152749938.

ABSTRACT

Surface water from the Rio Grande River is one of the primary water sources for southern New Mexico and Far West Texas in the United States (U.S.) and northern Chihuahua in Mexico. The river supplies several users, including agriculture, municipalities, industry, and wildlife. Surface water from precipitation, lakes, ponds, and swamps plays a significant role in the region's water supplies. However, climate change and the fast growth of the major metropolitan areas of El Paso, Ciudad Juárez, and Las Cruces have resulted in changes in land-use practices and increased water demand in response to growing competition between urban water needs and other uses. This study applies the Modified Normalized Difference Water Index (MNDWI) to visualize, monitor, and identify changes in surface water bodies in the Middle Rio Grande River Basin for a 26-year 1994-2020 study period. The area spans from San Antonio, New Mexico, to Presidio, Texas, and to Ojinaga, Chihuahua, including the cities of El Paso, Texas, Ciudad Juárez, Chihuahua, and Las Cruces, New Mexico, all metropolitan areas on the U.S.-Mexico border. Results show that surface waterbodies have experienced an overall decrease in surface area during the last twenty-six years by more than 66 percent. This decrease is especially evident for the Elephant Butte and Caballo reservoirs, which decreased by about 83 percent and 72 percent, respectively. In 2020, surface waterbodies increased by approximately 31.9 % compared to 2018 storage and reduced the surface water area decrease to 46.9 percent. Geographic information systems (GIS) and remote sensing (RS) proved useful tools for analyzing surface water change over time and monitoring mesoscale regions experiencing climate change, rapid urban growth, and water scarcity.

حساب التغير في الأجسام المائية السطحية في حوض وسط ريو جراندي عن طريق معامل إختلاف المياه المعدل 1994–2020

عمر سليمان بالحاج[1], ستنالي ت موباكو[2], كريج إي تويدي[3], رائد إي الدوري[4], وليم إل هارجروف[5], الهادي عبدالله هديه[6]

المياه السطحية من نهر ريوجراندي تعتبر من المصادر الأولية للمياه في جنوب ولاية نيو مكسيكو وأقصى غرب ولاية تكساس بالولايات المتحدة الأمريكية وشمال ولاية تشيواوا بالمكسيك. النهر يمد العديد من المستعملين بالمياه شاملاً قطاعات الزراعة والبلدية والصناعة والحياة البرية. المياه السطحية من الأمطار

Keywords:
Waterbodies, Modified Normalized Difference Water Index (MNDWI), environment, sustainability, ecosystems.

والبحيرات والمستنقعات تلعب دوراً هاماً في إمدادات المياه. تغير المناخ والنمو السريع للمناطق الحضرية في مدن الباسو وخوارس و لاسكرورسس أدى إلى تغيرات في إستعمالات الأراضي وزيادة الإحتياجات المائية لتلبية الإحتياجات المتنامية المتنافسة بين الإمدادات البلدية والقطاعات الأخرى. هذه الدراسة إستخدمت معامل إختلاف المياه المعدل لرؤية ومراقبة وتحديد التغيرات في أجسام المياه السطحية في حوض وسط نهر ريو جراندي لمدة 26 سنة (1994–2020). المنطقة تمتد من سان أنطونيو بولاية نيومكسيكو إلى بريسيديو بولاية تكساس وأوخيناجا بولاية تشيواوا شاملة مدن الباسو تكساس وخوارس تشيواوا ولاسكروسس نيومكسيكو على الحدود بين الولايات المتحدة الأمريكية والمكسيك. النتائج أوضحت أن أجسام المياه السطحية تعرضت لنفص في المساحة السطحية خلال الستة والعشرين سنة بأكثر من 66%. يظهر هذا النقص واضحاً خاصة في منطقة تخزين سدي إليفنت بيوت وكابيو اللذين تعرضا لنقص حوالي 83% و 72% على التوالي. في سنة 2020 الأجسام المائية السطحية تزايدت بحوالي 31.9% مقارنة بسنة 2018 لتصبح نسبة نقص المياه السطحية 46.9%. نظم المعلومات الجغرافية والإستشعار عن بعد تمثل أدوات مفيدة لمراقبة وتحليل تغيرالمياه السطحية عبر الزمن و مراقبة الأقاليم التي تتعرض لتغير المناخ والنمو السكاني السريع و نقص المياه.

INTRODUCTION:

Surface water is a crucial water resource for human existence and development (Li *et. al*., 2013; Acharya *et. al*., 2018; Varis *et. al*., 2019), as well as for animals, plants, and ecosystems (Huang *et. al*., 2018; Qin *et. al*., 2020). Its change is a significant indicator of environmental, meteorological, and anthropogenic actions (Zhai *et. al*., 2015; Acharya *et. al*., 2019). The deterioration of this resource increases poverty, insecurity, and biological diversity degradation (Campos *et. al*., 2012; Gupta, 2019; Abell *et. al*., 2019). Information on surface water amount and distribution is essential for surface water mapping, estimating quantities for drinking and irrigation purposes, land use/land cover, and monitoring change (Acharya *et. al*., 2019; Qin *et. al*., 2020). It also provides the capability to protect the environment and its components (Campos *et. al*., 2012; Gupta, 2019; Abell *et. al*., 2019). A vital rise in water uses throughout the twentieth century and through the first decades of this century has led to severe water scarcity in many regions around the world, and changes in mean hydro-climatological conditions under climate change potentially increase water scarcity in those regions (Greve *et. al*., 2018; Abell *et. al*., 2019). Many scientists and scholars have studied surface water bodies, and numerous methods have been established to delineate and study this landscape component (Yang *et. al*., 2017). Weather variability and climate change can potentially affect water availability, possibly negatively, resulting in a change in environmental sustainability (Gutzler, 2013; Mu *et. al*., 2018). However, population growth and increasing their demand for food, energy, and water could result from climate change in the long term (Gutzler, 2013; Mu *et. al*., 2018; Bohn *et. al*., 2018).factories, which can fragment MPs mechanically and discharge them into the ecosystem (Qi *et. al.*, 2020; Yang *et. al.*, 2021). Remote sensing and geographic information system technologies have been extensively used in various studies that include land use/cover change, urban growth, and aquatic resources (Li *et. al*., 2013; McFeeters, 2013; Rokni *et. al*., 2014; Butt *et. al*., 2015; Zhang *et. al*., 2016; Mubako *et. al*., 2018; Acharya *et. al*., 2018; Islam *et. al*., 2018). Remote sensing tools at different spatial, spectral, radiometric, and temporal resolutions offer a vast amount of data that have become significant sources for distinguishing, extracting, measuring, and reserving surface water bodies and their changes in recent times (Rokni *et. al*., 2014; Qiandong Guo *et. al*., 2017; Jason Yang & Xianrong Du, 2017; Tena *et. al*., 2019). Remote sensing has become a relatively low-cost source for feature detection and understanding of hydrogeological systems (Acharya *et. al*., 2019). Methods that have been developed and applied to identify, extract and measure waterbodies include (1) thematic classification (Zhai *et. al*., 2015; Acharya *et. al*., 2018; Huang *et. al*., 2018), (2) linear unmixing models (Burazerovic *et. al*., 2014; Huang *et. al*., 2018; *Jarchow et. al*., 2019), (3) single-band thresholding (Huang *et. al*., 2018; Mondejar *et. al*., 2019), and (4) applications of spectral water indices (Acharya *et. al*., 2018; Wang *et. al*., 2018; Huang *et. al*., 2018; Babaei *et. al*., 2019; Herndon *et. al*., 2020). Spectral water index methods, such as the normalized difference water index (NDWI) and modified normalized difference water index (MNDWI), which are calculated from one green-band image and one near-infrared (NIR) or shortwave infrared (SWIR) band image, can extract water body information more accurately, rapidly, and thoroughly than general feature classification methods (Li *et. al*., 2013; Babaei *et. al*., 2019). Water's important spectral characteristics are that it absorbs (NIR) radiation, transmits green and red lights, and allows for light reflection by features such as benthic sediments, aquatic plants, and other features (McFeeters 1996). On the other hand, vegetation and dry soil reflect NIR strongly. Based on these characteristics, either a single band or a ratio of two bands is typically used for water extraction (McFeeters 1996). For instance, density slicing to Landsat TM band 4 proved to

be an efficient method for extracting water bodies from rivers and lakes (Qiandong Guo *et. al*., 2017). The two band-method ratios usually use a visible band, such as green or red, divided by a NIR band. Therefore, water features are boosted while this process represses terrestrial vegetation and soil features. Using green and NIR bands, McFeeters (1996) proposed (NDWI) to extract open waterbodies. However, Xu (2006) used the modified normalized difference water index (MNDWI) algorithm to extract open water structures by replacing a NIR band with the SWIR band because the SWIR band spectral value of most land features is larger than that of the green band, but water feature is the opposite (Qiandong Guo *et. al*., 2017).

The Rio Grande River is the most crucial water source in the Rio Grande region and flows from north to south, providing essential water requirements to many sectors. It begins as a snow-fed stream high in the San Juan Luis Valley in southern Colorado. Otherwise, it makes the main surface water reservoirs in southern New Mexico, the Elephant Butte reservoir and the Caballo reservoir. By the time it reaches the border between New Mexico and Texas, it has taken on the color and composition of the farmlands watered on the south's route (Perez, 2001; Pascolini-Campbell *et. al*., 2017; Blythe *et. al*., 2018). This River is the fourth largest on the North American continent. It supports extensive irrigated agriculture as well as rapidly growing cities in three U.S. and five Mexican states. From El Paso, Texas, to the Gulf of Mexico, the river marks the international border between the U.S. and Mexico. Treaties for sharing the Rio Grande's water between the two countries and arrangements for joint management were concluded in 1906 and 1944 (Schmandt, 2002; Pascolini-Campbell *et. al*., 2017; Blythe *et. al*., 2018; Chavarria *et. al*., 2018). Furthermore, surface water from precipitation along the region and several unconventional water sources such as wastewater treatment facilities form some water lakes, ponds, and swamps in many places in the region, playing a significant role in water supplies. Changes in surface water due to climate change and the competing demands observed in the region, and a declining flow in the Rio Grande River make it imperative to monitor water resources and identify more management options (Pascolini-Campbell *et. al*., 2017; Chavarria *et. al*., 2018; Mu *et. al*., 2018; Overpeck *et. al*., 2020).

In this study, Modified Normalized Difference Water Index (MNDWI) was applied to Landsat images in order to attain these objectives:

1. Extract the surface waterbodies in the Middle Rio Grande Region.
2. Measure the surface area of surface waterbodies in this region.

Find the changes in the surface area of waterbodies in the 26 years 1994-2020.

The Study Area

The Middle Rio Grande Basin extends from near San Antonio, New Mexico, to Presidio, Texas, and Ojinaga, Chihuahua, along the Rio Grande River, with a length of about 592 km (367.7 miles) and various widths of between 63 km (39 miles) in the north around the Caballo Reservoir in south-central New Mexico to around 41 km (25.5 miles) near El Paso and Juarez to 37 km (22.9 miles) near Presidio and Ojinaga. The area of interest is located between north latitudes 340^0 $3^/$ $36^{//}$ and 290^0 $22^/$ $54^{//}$ and west longitudes 1070^0 $51^/$ $25^{//}$ and 1040^0 $12^/$ $56^{//}$ (Fig. 1). The total study area is 36,988 km^2 (14, 280 sq. miles) divided into six water sub-basins. This area includes three main metropolitan cities of El Paso (Texas, USA), Las Cruces (New Mexico, USA), and Ciudad Juárez (Chihuahua, Mexico), with some other small cities, towns, suburbs, and villages. In addition, intense irrigated agricultural activities are concentrated in the Rio Grande valley. The large dams of Caballo and Elephant Butte are the major surface water bodies in the area and are located in the northern part of the region delineated for this study (Fig. 1). The reservoirs are the main sources of surface water for the southern part of the study region. Shrublands and forests occupy the uplands and mountains surrounding the alluvial plain and are dominated by the Chihuahua desert ecosystem.

MATERIALS AND METHODS

The flowchart presented in Figure 2 below visualizes the RS and GIS techniques applied in this study. Key steps accomplished include data downloading and preparing, atmospheric correction, data clipping, minimum noise fraction transform (McFeeters, 2013; Rokni *et. al*., 2014; Liu *et. al*., 2016), and determination of MNDWI (Xu, 2006). This work was performed using the software ArcGIS 10.7.1 map, ArcGIS Online, ENVI 5.4, Microsoft Excel, and Google Earth.

- *Data collection*

Landsat images were downloaded from the U.S. Geological Survey (USGS) Earth Explorer and Global Visualization Viewer (GloVis) websites (http://earthexplorer.usgs.gov/, http://glovis.usgs.gov/) for the years 1994, 2000, 2005, 2010, 2015, 2018, and 2020 as shown in Figure 1. The following eight multispectral Landsat scenes cover the area of interest shown in Figure 1 (Path/Row): 031/039, 031/040, 032/038, 032/039, 033/037, 033/038, 034/036, and 034/037. Each scene had less than 10 percent cloud cover. Landsat 5 Thematic Mapper (TM) and Landsat 8 Operational Land Imager (OLI) provided the chosen area images. The dates for images ranged between the end of May and the first half of July, a period considered "leaf-on" in this study region. Dates for the Landsat 2020 images used in this study ranged between the end of March and the second half of April. Preparatory steps were performed, including extracting the images to the

study area boundaries, creating mosaics, and color correction. Also, atmospheric corrections and minimum noise fraction transform were made.

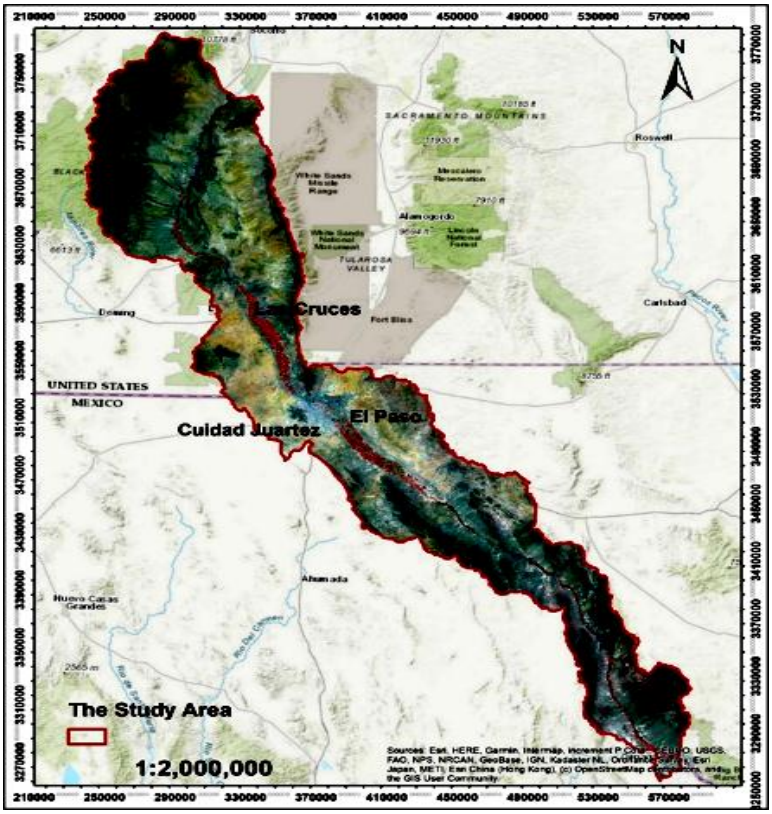

Figure 1. The study area.

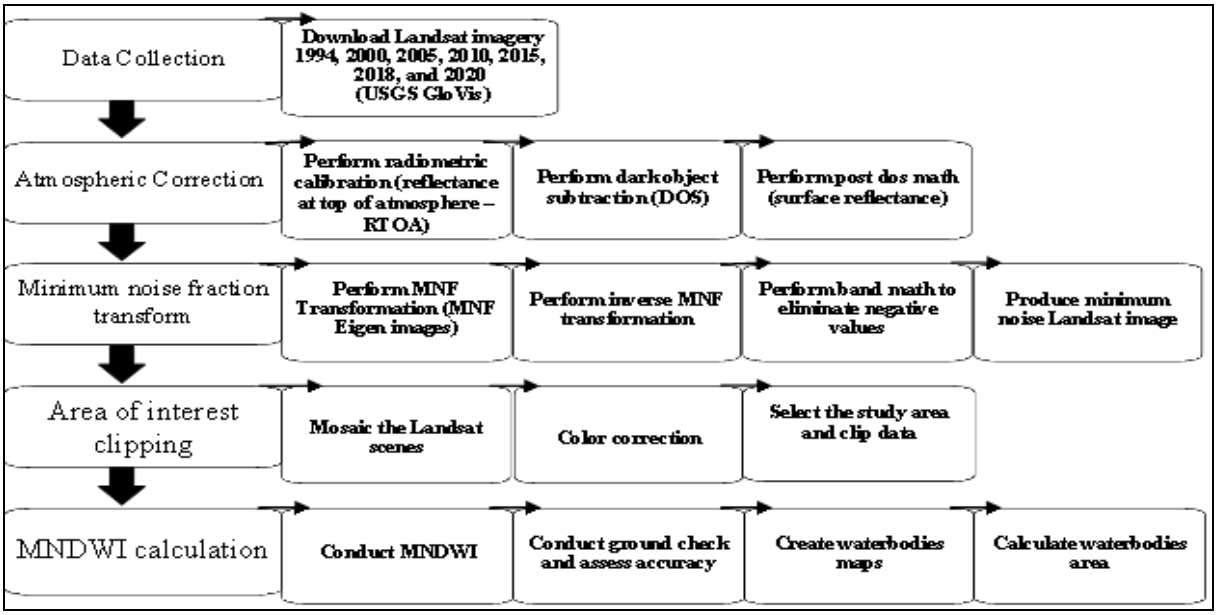

Figure 2. Flowchart showing RS and GIS technologies used in the study.

- *Modified Normalized Difference Water Index (MNDWI) Calculation*

In this study, MNDWI was calculated according to the procedure in Xu (2006). This index was developed to overcome the limits of NDWI (Gautam *et. al*., 2015; Acharya *et. al*., 2019). In MNDWI, the SWIR band (Landsat TM and ETM band 5, Landsat OLI band 6) was replaced the NIR band in McFeeters' NDWI equation to be the equation for calculating MNDWI is:

$$\mathbf{MNDWI} = \frac{(\boldsymbol{\rho}\mathbf{Green} - \boldsymbol{\rho}\mathbf{SWIR})}{(\boldsymbol{\rho}\mathbf{Green} + \boldsymbol{\rho}\mathbf{SWIR})}$$

Like McFeeters' NDWI, the threshold value for MNDWI was set to zero (Xu, 2006). However, Xu (2006) found a manual adjustment of the threshold could achieve more accurate results in the extraction of waterbodies (Ji *et. al*., 2009). ArcGIS software was used to calculate the MNDWI index using the Spatial Analyst Tool. The index was applied to all imagery in the seven analysis years.

- *Ground survey*

Field visits were undertaken to Elephant Butte and Caballo Reservoirs and other places along the Rio Grande River to check for similarities and differences between the classified features and their real locations using portable Global Positioning System (GPS) units. Coordinates and attributes of these places were also collected and assigned to familiar places through image visualization on Google Earth.

- *Accuracy Assessment*

To assess the accuracy of surface waterbodies extracted by MNDWI for the years 1994, 2000, 2005, 2010, 2015, 2018, and 2020 in the area of interest, and accuracy assessment of waterbodies extracted was conducted using the software ArcGIS 10.7.1. The study area was divided into two categories: waterbodies and non-waterbodies, and 500 sampling points were randomly generated in the study area with 250 points for each category. Each point was evaluated using high-resolution images (the US only) and/or Google Earth historical imagery.

Accuracy assessment was performed by building a confusion matrix for each interest region (Acharya *et. al*., 2019). The following five statistics were calculated: (1) Overall accuracy, representing the proportion of all correct classifications (2) Kappa coefficient, which measures the accuracy agreement in classification assessment. (3) User accuracy, which calculates the probability that a pixel classification is correct on the ground. (4) Producer accuracy, which is the probability that a pixel of a particular land-use type is assigned the correct land-use category (5) Omission error, which represents specific categories that were omitted when they exist on the ground and (6) Commission error, that represents categories that were identified as existing on the ground when in fact they do not (Feyisa *et. al*., 2014; Mubako *et. al*., 2018; Acharya *et. al*., 2019).

RESULTS AND DISCUSSION

- *4.1: Surface waterbodies areas, change, and trends*

MNDWI calculation results shown in Table 1, Figure 4, and Figure 5 generally show that surface waterbodies experienced a reduction in surface area during the 26 years 1994-2020 due to the increase in temperature trends and decrease in winter rains (Gutzler, 2013) and the reduction of snowpacks in the Rio Grande headwaters (Gutzler, 2013; Hargrove *et. al*., 2020). The total surface area decreased from 230.86 km^2 (89.14 sq. miles) in 1994 to 177.93 km^2 (68.70 sq. miles) in 2000, a 22.9 % decrease. It continued decreasing to 107.60 km^2 (41.54 sq. miles) in 2005, a 39.5 % decrease. It increased to 113.31 Km^2 (43.75 sq. miles) in 2010, a 5 % increase. However, it decreased to 86.52 km^2 (33.41 sq. miles) in 2015, 23.7 % for an overall decrease of 62.5 %. It also reduced from 86.52 km^2 (33.41 sq. miles) in 2015 to 76.63 km^2 (29.59 sq. miles) in 2018, an 11.4 % decrease during this time step and an overall reduction of 66.8 % for the time series. In the first half of 2020, it was found that surface water bodies increased to 112.5 km^2 (43.44 sq. miles), an increase of 31.9 % compared to 2018 storage. 2020 was an unusual year because after the melt of the high snowpack in river headwaters in 2018-2019, a significant irrigation user of water in Elephant Butte, the El Paso Water Improvement District #1, stored some of this good year in the reservoir rather than taking it all at once. In addition, and from the results, it was found that the surface water bodies experienced an overall decrease of 51.3 % for the 26 years of analysis.

Table 1. MNDWI results for the study area.

Year	Land use category area (km^2)		
	Waterbodies	Non waterbodies	Total Area
1994	230.86	36757.14	36988
2000	177.93	36810.07	36988
2005	107.60	36880.40	36988
2010	113.31	36874.69	36988
2015	86.52	36901.48	36988
2018	76.63	36911.37	36988
2020	112.50	36875.5	36988

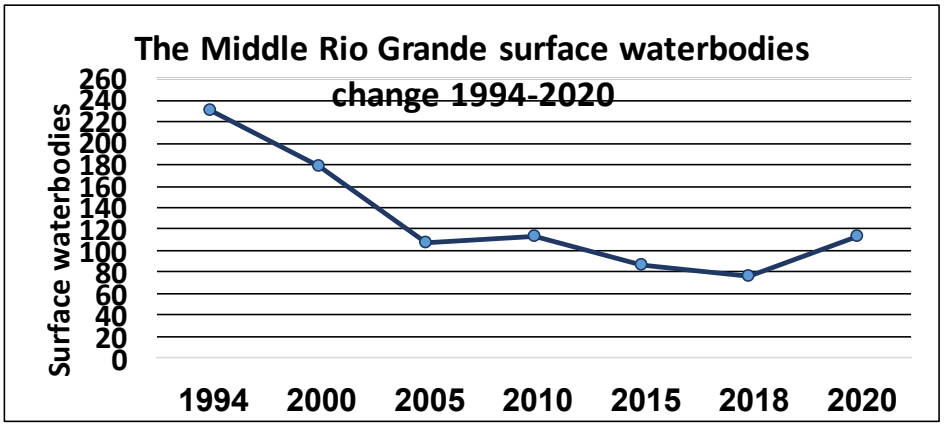

Figure 3. Middle Rio Grande Surface Waterbody change 1994-2020.

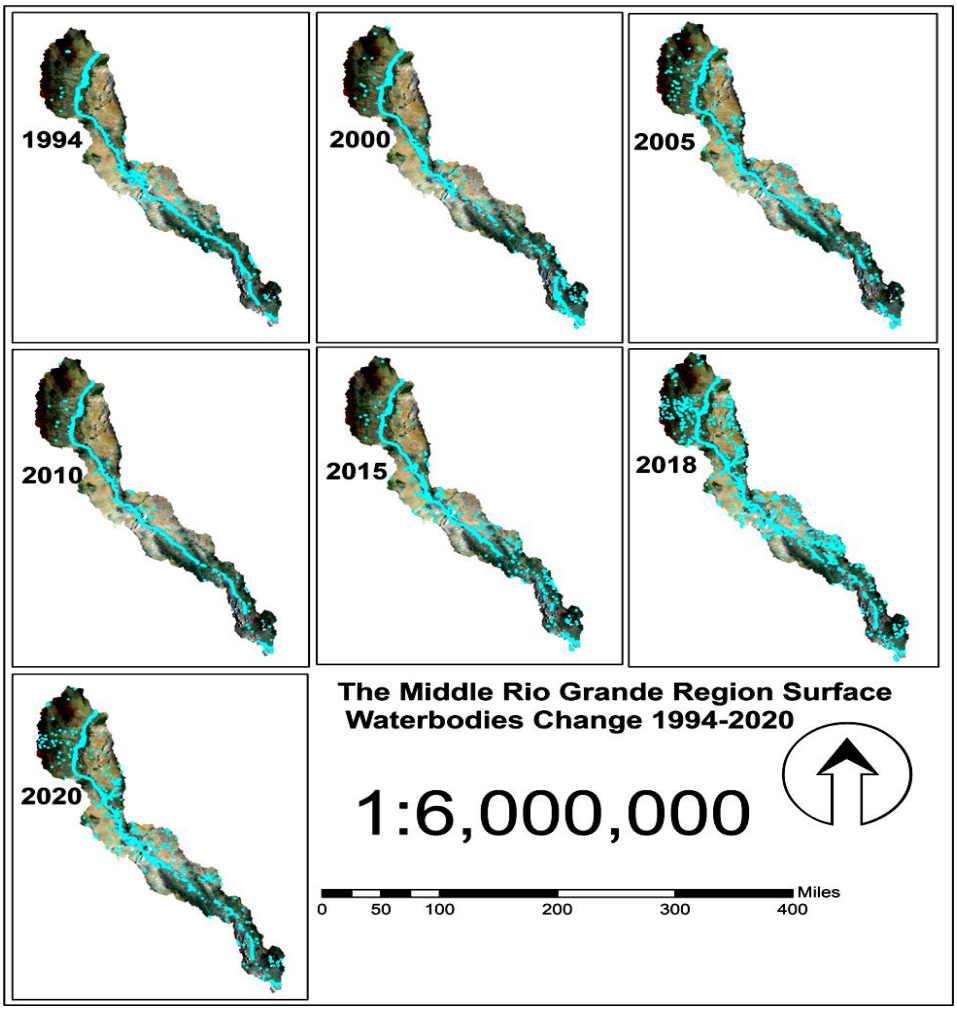

Figure 4. Middle Rio Grande Surface Waterbodies change 1994-2020.

Change of surface waterbodies storage in the region is evident in the main surface water reservoirs of Elephant Butte and Caballo Lakes, where water is accumulated and then allocated flow for the Rio Grande River water along the region. Changes in these reservoirs' storage are one of the most critical factors impacting water supplies downstream. While the rising storage of these water bodies justifies more allocations downstream to demanded sectors such as agriculture, the reduced storage causes meaningful cuts to allocations and shortages in meeting water demands. Moreover, as in Table (2), the surface area of the Elephant Butte reservoir decreased from 141 km^2 (54.4 sq. miles) in 1994 to 120.26 km^2 (46.43 sq. miles) in 2000, a decrease of 16.5 %. While it shrunk to 54 km^2 (20.8 sq. miles) in 2005, a 55 % Elephant Butte reservoir increased to 60.06 km^2 (23.19 sq. miles) in 2010 (11 % increase).

However, it decreased to 45 km^2 (17.4 sq. miles) in 2015, 16.7 %, for an overall decrease of 68 %. The surface area of this reservoir decreased from 45.17 km^2 (17.44 sq. miles) in 2015 to 24 km^2 (9.3 sq. miles) in 2018, a decrease of 45.9 % and an overall decrease of 83 % for the 26-year period. In 2020 and due to the reduction of water release, the Elephant Butte Reservoir's surface area increased to 50.03 km^2 (19.32 sq. miles), an increase of 51.4 % from what it was in 2018 to reduce the overall decrease to 65.3 %. Figures 5 and 7 show changes in surface area in the Elephant Butte reservoir.

Table 2. Elephant Butte and Caballo reservoirs surface water areas results.

Year	Surface area (km^2)	
	Elephant Butte	**Caballo**
1994	144.10	43.98
2000	120.26	26.78
2005	54.09	16.65
2010	60.06	21.15
2015	45.18	13.94
2018	24.43	12.32
2020	50.03	20.07

Caballo reservoir water storage decreased from 43 km^2 (16.6 sq. miles) surface area in 1994 to 26.78 km^2 (10.34 sq. miles) in 2000, a drop of 39.1 % to 16 km^2 (6.2 sq. miles) in 2005, a decline of 37.8 %. It increased to 21.15 km^2 (8.17 sq. miles) in 2010. However, Caballo's surface water area decreased to 14 km^2 (5.4 sq. miles) in 2015, 34.1 %, for an overall decrease of 68.3 % in the 26 years. Besides, it decreased from 14 km^2 (5.4 sq. miles) in 2015 to 12.32 km^2 (4.76 sq. miles) in 2018, an 11.3 % for an overall decrease of 72 % 26-year period. In 2020 and due to the reduction of water release, the Caballo Reservoir's surface area increased to 20.07 km^2 (7.75 sq. miles) by 37.5% from what it was in 2018 to reduce the overall decrease in water in this reservoir to 54.3 % in 26 years. Figures 6 and 8 show the change in surface area in the Caballo reservoir.

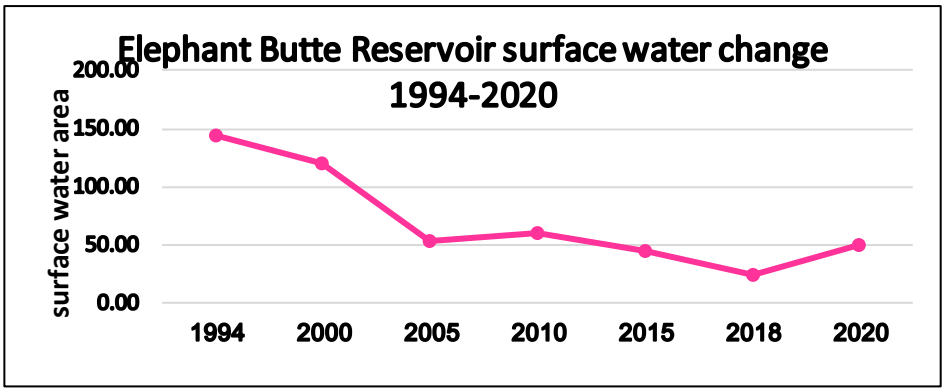

Figure 5. Elephant Butte Reservoir surface water change 1994-2020.

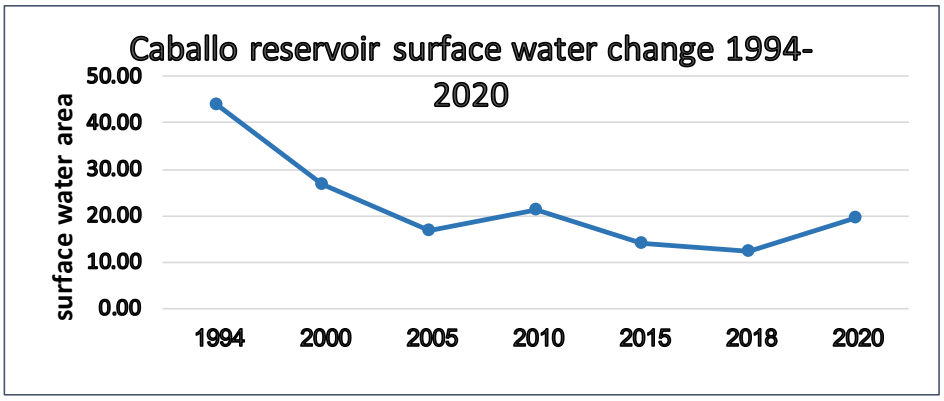

Figure 6. Caballo Reservoir surface water change 1994-2020.

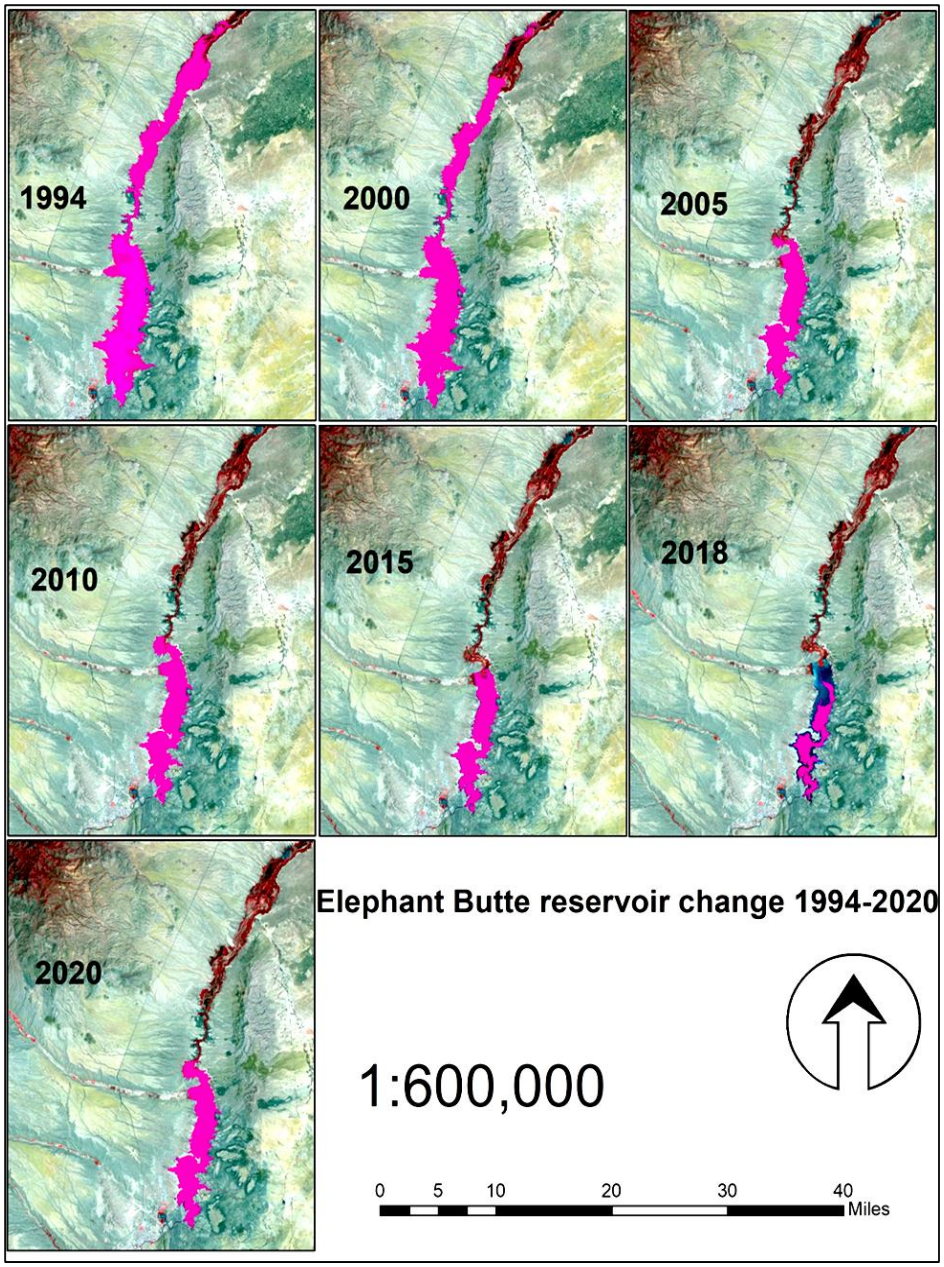

Figure 7. the Elephant Butte reservoir change 1994-2020

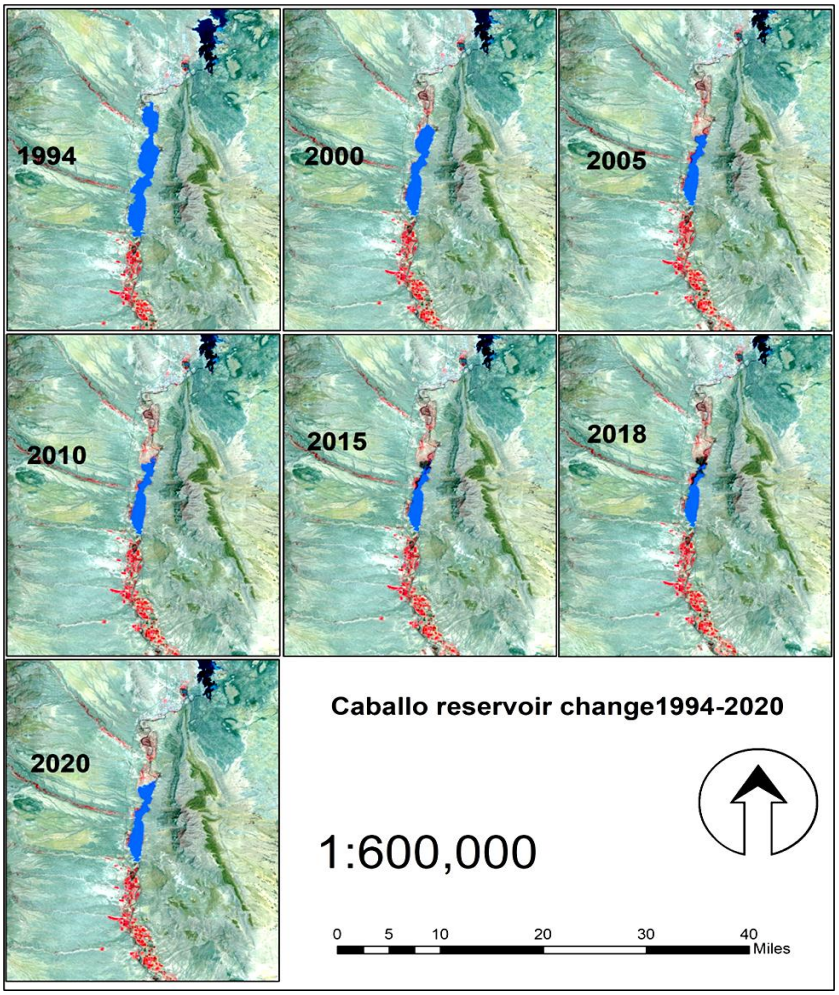

Figure 8. the Caballo reservoir change 1994-2020.

- *Accuracy assessment*

Confusion matrix

The results showed that MNDWI proposed in this study achieved the highest accuracy with the best visual effect in water extraction. We detail accuracy assessment results for the area of interest, focusing on analysis years 2010, 2015, and 2018. The MNDWI method's quality is provided in a confusion matrix, a widely used tool to present accuracy assessment information in remote sensing (Tilahun *et. al*., 2015; Mubako *et. al*., 2018). The overall accuracy was 98 percent in 2010. The Kappa coefficient was 0.96, the producer accuracy ranged from 96 percent to 100 percent for 2010, and the user accuracy also ranged from 96 to 100 percent (Table 3).

The overall accuracy was 96 percent in 2015. The Kappa coefficient was 0.92, the producer accuracy ranged from 92 percent to 100 percent for 2015, and user accuracy from 92 to 100 percent (Table 4).

The overall accuracy was 97 percent in 2018. The Kappa coefficient was 0.95, the producer accuracy ranged from 95 percent to 100 percent for 2018, and user accuracy also ranged from 95 to 100 percent (Table 5).

Table 3. Confusion matrix for 2010 image showing classification accuracy and errors.

Classified category	Actual category: Ground truth				
	Waterbodies	Nonwaterbodies	Total number of samples	User accuracy %	The error of commission %
Water	250	0	250	100	0
Nonwaterbodies	10	240	250	96	4
Total	260	240	500		
Producer accuracy %	96	100	Overall accuracy % 98		
The error of omission %	4	0	Kappa coefficient 0.96		

Table 4. Confusion matrix for 2015 image showing classification accuracy and error.

	Actual category: Ground truth				
Classified category	Waterbodies	Nonwaterbodies	Total number of samples	User accuracy %	The error of commission %
Water	250	0	250	100	0
Nonwaterbodies	21	229	250	92	4
Total	271	229	500		
Producer accuracy %	92	100	Overall accuracy % 96		
The error of omission %	4	0	Kappa coefficient 0.92		

Table 5. Confusion matrix for 2018 image showing classification accuracy and error.

	Actual category: Ground truth				
Classified category	Waterbodies	Nonwaterbodies	Total number of samples	User accuracy %	The error of commission %
Water	250	0	250	100	0
Nonwaterbodies	13	237	250	95	5
Total	263	237	500		
Producer accuracy %	95	100	Overall accuracy % 97		
The error of omission %	5	0	Kappa coefficient 0.95		

The overall classification accuracy for both classes of the study is more than 75-85 percent, which is acceptable, as stated in GIS studies, and supports that accuracy assessment is a compromise between perfect and confident (Keranen and Kolvoord, 2014; Wondrade *et. al*., 2014, Mubako *et. al*., 2018). The overall classification accuracy should be in the range of 84-85 percent for most satellite data classification studies (Wickham, 2013). User and producer accuracy results were thus reasonable. Another method of confirming classification accuracy is calculating the Kappa coefficient. The Kappa coefficient commonly underestimates overall accuracy and is recommended for vegetation mapping (Congalton and Green, 1999; Akasheh *et. al*., 2008). Accurate reference data are essential for testing classification accuracy (Martin *et. al*., 2014). Therefore, our results classification errors are partly due to the uncertainty of some water features along the river, especially in flatter areas and locations where shallow waterbodies or wetlands exist. These areas are covered by shrublands, grown vegetation, or suspended materials whose features overlap with water features. This overtopping was observed mostly in areas where features were smaller than the spatial resolution and were reimaged in the wrong pixel of the raster data. Errors in results were calculated using omissions and commissions, which were found from 0 to 5%.

Field survey

The collected coordinates and the assigned points were checked and matched with the produced maps. These points did not cover the whole study area because that was not practical, but the results gave more confidence to MNDWI calculations.

HydroData comparison

As an additional process to confirm the accuracy of the MNDWI results, we compared the results of the surface areas for Elephant Butte and Caballo reservoirs with HydroData, which is the U.S. Bureau of Reclamation's hydrologic database access portal that provides Reservoir data (including storage, inflow, releases, elevation, and more), Gage data (flow, flow volume, and side inflows), and Basin maps (including current reservoir capacity and current and historical snow and precipitation charts) (https://www.usbr.gov/uc/water/hydrodata/nav.html).

Table 6 expresses the comparative results of MNDWI and HydroData of Elephant Butte reservoir at the exact date of the requisitioned Land sat data used in this study as in figure 3. The results indicate that the Elephant Butte reservoir's surface area matched 87.41% of the HydroData results.

Table 6. Comparison between MNDWI and HydroData of Elephant Butte Reservoir.

Class / Year	Waterbodies measured km^2	% Period change	% Total change	Waterbodies estimated (HydroData) km^2	Difference	% Difference	%Accuracy of MNDWI
1994	**144.10**			**140.24**	**3.86**	**2.68**	**97.32**
2000	**120.26**	**-16.50**	**-16.50**	**115.48**	**4.78**	**3.97**	**96.03**
2005	**54.09**	**-55.00**	**-62.50**	**51.94**	**2.15**	**3.97**	**96.03**
2010	**60.06**	**11.00**	**-58.30**	**58.90**	**1.16**	**1.92**	**98.08**
2015	**45.18**	**-24.80**	**-68.65**	**45.82**	**-0.64**	**-1.42**	**98.58**
2018	**24.43**	**-45.90**	**-83.00**	**39.34**	**-14.91**	**-61.02**	**38.98**
2020	**50.03**	**57.69**	**-59.93**	**43.46**	**6.57**	**13.14**	**86.86**
The average accuracy							87.41

Table 7 expresses the comparative results of MNDWI and HydroData for Caballo reservoir at the exact date of the requisitioned Land sat data used in this study, as in Figure 3. The results indicate that the surface area of the Caballo reservoir matched 91.76% of the HydroData results.

Table 7: Comparison between MNDWI and HydroData of Caballo reservoir.

Class / Year	Waterbodies measured km2	% Period change	% Total change	Waterbodies estimated (HydroData) km2	Difference	% Difference	%Accuracy of MNDWI
1994	**43.98**			**43.91**	**0.07**	**0.16**	**99.84**
2000	**26.78**	**-39.10**	**-39.10**	**21.47**	**5.32**	**19.85**	**80.15**
2005	**16.65**	**-37.80**	**-62.10**	**15.63**	**1.03**	**6.15**	**93.85**
2010	**21.15**	**27.00**	**-51.90**	**17.39**	**3.76**	**17.79**	**82.21**
2015	**13.94**	**-34.10**	**-68.30**	**13.54**	**0.40**	**2.89**	**97.11**
2018	**12.32**	**-11.30**	**-72.00**	**12.52**	**-0.21**	**-1.69**	**98.31**
2020	**20.07**	**40.31**	**-53.08**	**21.91**	**-1.84**	**-9.16**	**90.84**
The average accuracy							91.76

CONCLUSION:

This study applied modified normalized difference water index MNDWI as remote sensing and geographic information systems techniques to visualize, extract, measure, and assess surface water feature alteration in the Middle Rio Grande region in the 26 years 1994-2020.

Results show that surface aquatic features have decreased by more than 66 percent from 1994 until 2018. The main water reservoirs of the Elephant Butte reservoir decreased by 83 percent, and the Caballo reservoir decreased by 72 percent. Moreover, in 2020, the surface water area ended with a reduction of 46.9 percent after saving reasonable amounts of water in the 2018 and 2019 seasons. The storage of the two reservoirs ended with a decrease of 59 percent in the Elephant Butte reservoir and 53 in the Caballo reservoir. The study results are valuable outcomes that will help understand the spatial and temporal aspects of surface water and its change in this region and support stakeholders and decision-makers manage this precious component better.

These results bring up some important questions that need to be answered, like what will the future of surface water extent in the region? What are the implications of surface water reduction on future settlement in the region? What are the consequences of surface water reduction on biodiversity and sustainability in the region? What are the impacts of surface water reduction on the ecological systems in and around the Elephant Butte and Caballo reservoirs? Is there any way to mitigate the change of waterbodies areas?

This study recommended some changes and improvements in water use and conservation. Because of the large surface area of the Elephant Butte and the Caballo reservoirs, there is a need to work toward reducing evaporation rates by covering their surface. Since most farming lands use flood irrigation methods that consume vast amounts of water, shifting to more efficient and less water consumption methods such as

sprinkler and drip methods is better. Because agriculture consumes an immense amount of water, changing agriculture practices to less using water crops is the better solution to preserve water. Policy changes to better water use practices that sustain this resource and extend its existence. Implementing more scientific research on the driving forces behind surface water change and the deficit of its needs that Hargrove *et. al*. demonstrated in 2020 be conducted, which are: decreased snowpack and changed flows times in the headwaters of the Rio Grande/Rio Bravo, increasing temperatures and evapotranspiration rates, change of agricultural practices toward high water demand crops, increasing salinity in water sources and soils, and urban growth in the river area.

Acknowledgements :

This study was made possible through support from the National Institute of Food and Agriculture, U.S. Department of Agriculture, under award number 2015-68007-23130. The opinions in this paper are those of the authors and do not necessarily reflect the USDA's views. The authors would like to acknowledge valuable comments and inputs from various collaborators on the USDA-NIFA project.

REFERENCES

Abell, R., Vigerstol, K., Higgins, J., Kang, S., Karres, N., Lehner, B., ... & Chapin, E. (2019). Freshwater biodiversity conservation through source water protection: Quantifying the potential and addressing the challenges. Aquatic Conservation: Marine and Freshwater Ecosystems, 29(7), 1022-1038.

Akasheh, O. Z., Neale, C. M., & Jayanthi, H. (2008). Detailed mapping of riparian vegetation in the middle Rio Grande River using high resolution multi-spectral airborne remote sensing. Journal of Arid Environments, 72(9), 1734-1744.

Acharya, T. D., Subedi, A., & Lee, D. H. (2018). Evaluation of water indices for surface water extraction in a Landsat 8 scene of Nepal. *Sensors*, *18*(8), 2580.

Acharya, T. D., Subedi, A., Huang, H., & Lee, D. H. (2019). Application of Water Indices in Surface Water Change Detection using Landsat Imagery in Nepal. *Sens. Mater*, *31*, 1429-1447.

Atwah, W. (2021). Land Use and Land Cover Change Impact On Sustainability In The United Arab Emirates: A Big-Data Approach Using Google Earth Engine.

Babaei, H., Janalipour, M., & Tehrani, N. A. (2019). A simple, robust, and automatic approach to extract water body from Landsat images (case study: Lake Urmia, Iran). Journal of Water and Climate Change.

Blythe, T. L., & Schmidt, J. C. (2018). Estimating the natural flow regime of rivers with long- standing development: The northern branch of the Rio Grande. Water Resources Research, 54(2), 1212-1236.

Bohn, T. J., Vivoni, E. R., Mascaro, G., & White, D. D. (2018). Land and water use changes in the US–Mexico border region, 1992–2011. Environmental Research Letters, 13(11), 114005.

Burazerović, D., Heylen, R., Raymaekers, D., Knaeps, E., Philippart, C. J., & Scheunders, P. (2014). A Spectral-Unmixing Approach to Estimate Water–Mass Concentrations in Case 2 Waters. IEEE Journal of Selected Topics in Applied Earth Observations and Remote Sensing, 7(8), 3595-3605.

Butt, A., Shabbir, R., Ahmad, S. S., & Aziz, N. (2015). Land use change mapping and analysis using Remote Sensing and GIS: A case study of Simly watershed, Islamabad, Pakistan. *The Egyptian Journal of Remote Sensing and Space Science*, *18*(2), 251-259.

Campos, J. C., Sillero, N., & Brito, J. C. (2012). Normalized difference water indexes have dissimilar performances in detecting seasonal and permanent water in the Sahara–Sahel transition zone. *Journal of Hydrology*, *464*, 438-446.

Chavarria, S. B., & Gutzler, D. S. (2018). Observed changes in climate and streamflow in the upper Rio Grande Basin. JAWRA Journal of the American Water Resources Association, 54(3), 644-659.

Congalton, R. G. and Green, K. 1999. Assessing the Accuracy of Remotely Sensed Data: Principles and Practices, Boca Raton, FL: Lewis Publishers.

Feyisa, G. L., Meilby, H., Fensholt, R., & Proud, S. R. (2014). Automated Water Extraction Index: A new technique for surface water mapping using Landsat imagery. *Remote Sensing of Environment*, *140*, 23-35.

Gautam, V. K., Gaurav, P. K., Murugan, P., & Annadurai, M. (2015). Assessment of surface water Dynamicsin Bangalore using WRI, NDWI, MNDWI, supervised classification and KT transformation. *Aquatic Procedia*, *4*, 739-746.

Greve, P., Kahil, T., Mochizuki, J., Schinko, T., Satoh, Y., Burek, P., ... & Wada, Y. (2018). Global assessment of water challenges under uncertainty in water scarcity projections. Nature Sustainability, 1(9), 486-494.

Gupta, G. S. (2019). Land degradation and challenges of food security. Rev. Eur. Stud., 11, 63.

Gutzler, D. S. (2013). Regional climatic considerations for borderlands sustainability. Ecosphere, 4(1), 1-12.

Haibo, Y., Zongmin, W., Hongling, Z., & Yu, G. (2011). Water body extraction methods study based on RS and GIS. *Procedia Environmental Sciences*, *10*, 2619-2624.

Hargrove, W. L., & Heyman, J. M. (2020). A Comprehensive Process for Stakeholder Identification and Engagement in Addressing Wicked Water Resources Problems. Land, 9(4), 119.

Herndon, K., Muench, R., Cherrington, E., & Griffin, R. (2020). An Assessment of Surface Water Detection Methods for Water Resource Management in the Nigerien Sahel. Sensors, 20(2), 431.

Huang, C., Chen, Y., Zhang, S., & Wu, J. (2018). Detecting, extracting, and monitoring surface water from space using optical sensors: A review. Reviews of Geophysics, 56.

Islam, K., Jashimuddin, M., Nath, B., & Nath, T. K. (2018). Land use classification and change detection by using multi-temporal remotely sensed imagery: The case of Chunati wildlife sanctuary, Bangladesh. *The Egyptian Journal of Remote Sensing and Space Science*, *21*(1), 37-47.

Jarchow, C. J., Sigafus, B. H., Muths, E., & Hossack, B. R. (2019). Using Full and Partial Unmixing Algorithms to Estimate the Inundation Extent of Small, Isolated Stock Ponds in an Arid Landscape. Wetlands, 1-13.

Jason Yang & Xianrong Du (2017) An enhanced water index in extracting water bodies from Landsat TM imagery, Annals of GIS, 23:3, 141-148, DOI: 10.1080/19475683.2017.1340339.

Ji, L., Zhang, L., & Wylie, B. (2009). Analysis of dynamic thresholds for the normalized difference water index. Photogrammetric Engineering & Remote Sensing, 75(11), 1307-1317.

Keranen, K., & Kolvoord, R. (2014). *Making Spatial Decisions Using GIS and Remote Sensing: A Workbook*. Esri Press.

Li, W., Du, Z., Ling, F., Zhou, D., Wang, H., Gui, Y., … Zhang, X. (2013). A Comparison of Land Surface Water Mapping Using the Normalized Difference Water Index from TM, ETM+ and ALI. Remote Sensing, 5(11), 5530–5549. doi:10.3390/rs5115530.

Liu, B., Li, Y., Chen, P., & Zhu, X. (2016). Extraction of oil spill information using decision tree based minimum noise fraction transform. *Journal of the Indian Society of Remote Sensing*, *44*(3), 421-426.

McFeeters, S. K. (1996). The use of the Normalized Difference Water Index (NDWI) in the delineation of open water features. *International journal of remote sensing*, *17*(7), 1425-1432.

McFeeters, S. (2013). Using the Normalized Difference Water Index (NDWI) within a Geographic Information System to Detect Swimming Pools for Mosquito Abatement: A Practical Approach. *Remote Sensing*, *5*(7), 3544–3561. doi:10.3390/rs5073544.

Martin, R., Brabyn, L., & Beard, C. (2014). Effects of class granularity and cofactors on the performance of unsupervised classification of wetlands using multi-spectral aerial photography. *Journal of Spatial Science*, *59*(2), 269-282.

Mondejar, J. P., & Tongco, A. F. (2019). Near infrared band of Landsat 8 as water index: a case study around Cordova and Lapu-Lapu City, Cebu, Philippines. Sustainable Environment Research, 29(1), 16.

Mu, J. E., & Ziolkowska, J. R. (2018). An integrated approach to project environmental sustainability under future climate variability: An application to US Rio Grande Basin. Ecological Indicators, 95, 654-662.

Mubako, S., Belhaj, O., Heyman, J., Hargrove, W., & Reyes, C. (2018). Monitoring of Land Use/Land-Cover Changes in the Arid Transboundary Middle Rio Grande Basin Using Remote Sensing. *Remote Sensing*, *10*(12), 2005.

Overpeck, J. T., & Udall, B. (2020). Climate change and the aridification of North America. Proceedings of the National Academy of Sciences, 117(22), 11856-11858.

Pascolini-Campbell, M., Seager, R., Pinson, A., & Cook, B. I. (2017). Covariability of climate and streamflow in the Upper Rio Grande from interannual to interdecadal timescales. Journal of Hydrology: Regional Studies, 13, 58-71.

Perez, A. E. (2000). Satellite Detection of Land Use Changes in The Rio Grande Valley from Elephant Butte Dam, NM, To Fort Quitman, TX.

Qiandong Guo, Ruiliang Pu, Jialin Li & Jun Cheng (2017) A weighted normalized difference water index for water extraction using Landsat imagery, International Journal of Remote Sensing, 38:19, 5430-5445, DOI: 10.1080/01431161.2017.1341667.

Qin, Y., Abatzoglou, J. T., Siebert, S., Huning, L. S., AghaKouchak, A., Mankin, J. S., ... & Mueller, N. D. (2020). Agricultural risks from changing snowmelt. Nature Climate Change, 10(5), 459-465.

Rokni, K., Ahmad, A., Selamat, A., & Hazini, S. (2014). Water feature extraction and change detection using multitemporal Landsat imagery. *Remote sensing*, *6*(5), 4173-4189.

Schmandt, J. (2002). Bi-national water issues in the Rio Grande/Rıo Bravo basin. *Water Policy*, *4*(2), 137-155.

Tena, T. M., Mwaanga, P., & Nguvulu, A. (2019). Impact of land use/land cover change on hydrological components in Chongwe River Catchment. Sustainability, 11(22), 6415.

Tilahun, A., & Teferie, B. (2015). Accuracy assessment of land use land cover classification using Google Earth. *American Journal of Environmental Protection*, *4*(4), 193-198.

Varis, O., Taka, M., & Kummu, M. (2019). The Planet's Stressed River Basins: Too Much Pressure or Too Little Adaptive Capacity? Earth's Future, 7(10), 1118-1135.

Wang, X., Liu, S., Du, P., Liang, H., Xia, J., & Li, Y. (2018). Object-based change detection in urban areas from high spatial resolution images based on multiple features and ensemble learning. Remote Sensing, 10(2), 276.

Wickham, J. D., Stehman, S. V., Gass, L., Dewitz, J., Fry, J. A., & Wade, T. G. (2013). Accuracy assessment of NLCD 2006 land cover and impervious surface. *Remote Sensing of Environment*, *130*, 294-304.

Wondrade, N., Dick, Ø. B., & Tveite, H. (2014). GIS based mapping of land cover changes utilizing multi-temporal remotely sensed image data in Lake Hawassa Watershed, Ethiopia. *Environmental monitoring and assessment*, *186*(3), 1765-1780.

Xie, H., Luo, X., Xu, X., Pan, H., & Tong, X. (2016). Evaluation of Landsat 8 OLI imagery for unsupervised inland water extraction. International Journal of Remote Sensing, 37(8), 1826-1844.

Xu, H., 2006. Modification of normalized difference water index (NDWI) to enhance open water features in

remotely sensed imagery, *International Journal of Remote Sensing*, 27(14):3025–3033.

Yang, J., & Du, X. (2017). An enhanced water index in extracting water bodies from Landsat TM imagery. *Annals of GIS*, *23*(3), 141-148.

Zhai, K., Wu, X., Qin, Y., & Du, P. (2015). Comparison of surface water extraction performances of different classic water indices using OLI and TM imageries in different situations. *Geo-spatial Information Science*, *18*(1), 32-42.

Zhang, F., Li, J., Shen, Q., Zhang, B., Ye, H., Wang, S., & Lu, Z. (2016). Dynamic Threshold Selection for the Classification of Large Water Bodies within Landsat-8 OLI Water Index Images. *Remote Sens*.